

SPATIO-TEMPORAL CROP CLASSIFICATION ON VOLUMETRIC DATA

Muhammad Usman Qadeer, Salar Saeed, Murtaza Taj and Abubakr Muhammad

ABSTRACT

Large-area crop classification using multi-spectral imagery is a widely studied problem for several decades and is generally addressed using classical Random Forest classifier. Recently, deep convolutional neural networks (DCNN) have been proposed. However, these methods only achieved results comparable with Random Forest. In this work, we present a novel CNN based architecture for large-area crop classification. Our methodology combines both spatio-temporal analysis via 3D CNN as well as temporal analysis via 1D CNN. We evaluated the efficacy of our approach on Yolo and Imperial county benchmark datasets. Our combined strategy outperforms both classical as well as recent DCNN based methods in terms of classification accuracy by 2% while maintaining a minimum number of parameters and the lowest inference time.

Index Terms— Satellite data, CNN, Crop Classification

1. INTRODUCTION

The freely available multispectral satellite imagery and advancement in modern machine learning have paved the way for a wide variety of applications. These include disaster assessment [1], crop classification [2, 3], urbanization [4] and environment monitoring [5]. The increasing quality and resolution of available remote sensing imagery have made it possible to perform robust crop monitoring and yield estimation over large areas [6]. For instance, the Sentinel-2 satellite imagery with a spatial resolution of 10m and Landsat-8 imagery with a spatial resolution of 30m is available every five days and 16 days, respectively. Thus, enabling us to perform detailed spatio-temporal analysis [7].

Supervised learning is considered to be the state-of-the-art approach to produce crop maps. Some traditional machine learning algorithms like Support Vector Machines (SVM) [8], K-nearest neighbors (KNN) [9], Cart [10], and Random Forest [11] have been widely applied for crop classification. Among these methods, those using a series of images at different time stamps [12] have shown better results than the one using a single image [8].

Due to the popularity of deep learning, recently, the problem of crop classification has also been attempted using different deep learning architectures. In earlier work, a 1D convolutional neural network model has been proposed [13] which stacked features of different time stamps as in the case

of random forest. To use the temporal information more efficiently, [14] has proposed a new 1D CNN model. This method feeds multivariate time series to 1D CNN instead of stacked values of features. Similarly, a new 1D CNN architecture based on the idea of the Inception network has been introduced [15]. It has shown improved performance on traditional machine learning algorithms, including Random Forest and XGboost [16].

The 2D convolutional neural networks show outstanding image classification performance, and many architectures, including Alexnet [17], Inception, Resnets [18], etc., have been introduced. A new dataset comprising Sentinel-2 images of different landcover types from around the world has been developed [19] and different 2D CNN architectures, including Resnet50 and GoogleNet [20], have been compared to classify the multispectral images. Recently, an ensemble of 2D CNN has been used for crop classification using multi-temporal Sentinel-1 and Landsat-8 imagery [21]. This study shows the significance of using spatial information in addition to temporal one.

The recurrent neural networks are very popular for applications where time-series data is used. The idea of using LSTM [22] has also been applied to landcover classification using multi-temporal SAR imagery [15]. This work has claimed that LSTM performs worse than Random Forest classifier for crop classification using multispectral imagery. The recurrent convolutional neural network (R-CNN) [23] uses LSTM followed by 2D CNN, but unlike [21], this architecture uses the information of only one pixel. The idea of combining CNN and LSTM has also been introduced for landcover classification [24][25].

The 3D convolutional neural networks are widely considered for applications related to video, medical imaging, and remote sensing [26]. In [27], a 3D CNN architecture has been presented showing better performance than 2D CNN as it uses the temporal information better than the 2D CNN where timestamps of all features are stacked on one axis.

Existing literature suggests various ways to exploit available spatio-temporal data [26, 27] however, these methods are either good at utilizing spatial information or temporal information but not both. We instead propose a novel DCNN based architecture that combines both spatial as well as temporal analysis. In the first stage of our architecture, we propose to use 3D convolutions that perform spatio-temporal analysis without collapsing the temporal dimension. Once

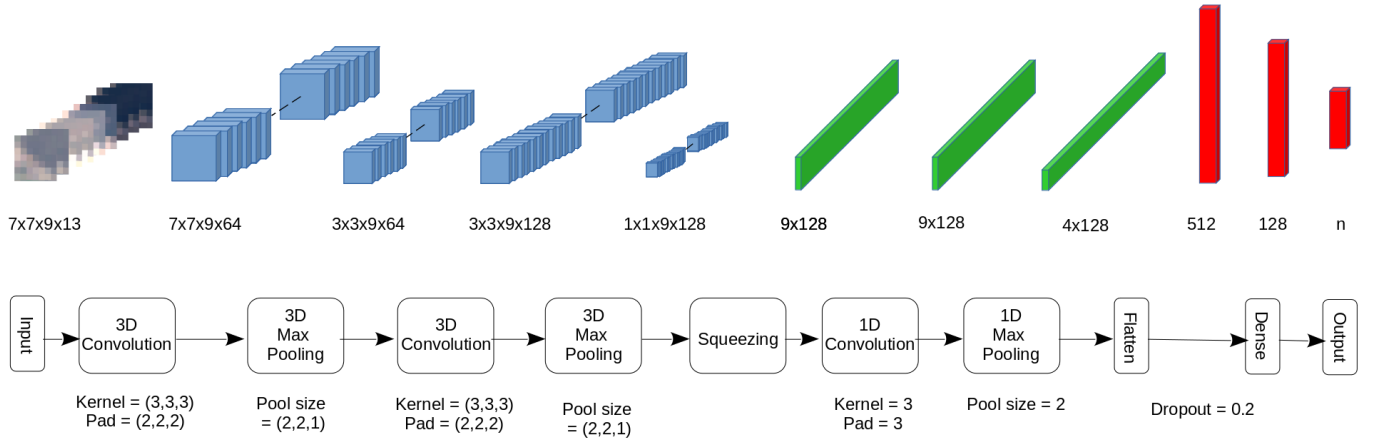


Fig. 1. Proposed model architectures showing combination of spatio-temporal and temporal convolution blocks. Spatio-temporal block via 3D CNN are shown in blue whereas the temporal only block via 1D convolution are shown in green.

the spatio-temporal features are extracted via multiple 3D CNN layers, we introduce temporal only analysis to further extract important information from the temporal dimension only. This spatio-temporal followed by temporal only analysis helps eliminate noise, usually present in the temporal only analysis. Thus the proposed approach outperforms classical as well as state-of-art-methods on benchmark datasets.

2. METHODOLOGY

2.1. Data Pre-processing

We have divided the pre-processing of data into five steps. The first step is to select all the images of a multispectral satellite for the region of interest in a suitable period, covering every crop's cropping season under consideration. For this purpose, the NDVI time series for different crops have been examined. The second step is to select the least cloudy images in that period. In our case, the images with cloud cover less than 10% have been selected. The third step is the cloud masking of the chosen images. The fourth step is to take the median of images chosen for each month. This step is for larger areas, as in our case, because the region can't be covered in a single image of a satellite. In the fifth and final step, the missing pixels due to the cloud or other reasons have been filled, which can be done using simple interpolation or linear regression. All these pre-processing steps have been performed on the Google Earth Engine Platform.

2.2. Feature Selection

For each image in our dataset, 13 features have been selected. The selected features have six multi-spectral satellite imagery bands, including Blue, Green, Red, Near Infrared (NIR), and two Short Wave Infrared (SWIR) bands. Table 1 shows the selected Sentinel-2 and Landsat-8 bands. The other seven features are indices derived from these bands, including Normalized Difference Vegetation Index (NDVI), Enhanced Vegetation Index, Green Normalized Difference Vegetation

Index (GNDVI), Soil Adjusted Vegetation Index (SAVI), Bare Soil Index (BSI), Normalized Difference Water Index (NDWI) and Normalized Difference Buildup Index (NDBI). These indices [28, 29] are calculated as follows:

$$\text{NDVI} = \frac{\text{NIR} - \text{RED}}{\text{NIR} + \text{RED}}, \quad \text{GNDVI} = \frac{\text{NIR} - \text{GREEN}}{\text{NIR} + \text{GREEN}}$$

$$\text{EVI} = 2.5 \times \frac{\text{NIR} - \text{RED}}{\text{NIR} + 6 \times \text{RED} - 7.5 \times \text{BLUE} + 1}$$

$$\text{SAVI} = 1.5 \times \frac{\text{NIR} - \text{RED}}{\text{NIR} + \text{RED} + 0.5}$$

$$\text{BSI} = \frac{(\text{SWIR} + \text{RED}) - (\text{NIR} + \text{BLUE})}{(\text{SWIR} + \text{RED}) + (\text{NIR} + \text{BLUE})}$$

$$\text{NDBI} = \frac{\text{SWIR1} - \text{NIR}}{\text{SWIR1} + \text{NIR}}, \quad \text{NDWI} = \frac{\text{GREEN} - \text{NIR}}{\text{GREEN} + \text{NIR}}$$

2.3. Model Architecture

The model architecture is shown in Fig. 1. The model consists of three parts concatenated to each other. The first part shown in blue performs spatio-temporal convolution using 3D CNN. The second part shown in green performs the temporal convolution. The output of 3D CNN is squeezed before feeding to 1D CNN. These two parts extract the features from input. The third part consists of a fully connected neural network, which predicts the label from multi-temporal input images.

The model input shape is (r, r, t, c) where r is the spatial dimension of input, t is the number of timestamps, and c is the number of channels. In our implementation, spatial dimension r is 7, timestamps t are 9 and channels c are 13. Each convolutional block has a batch normalization layer before activation. It has been observed that with batch-normalization, the model converges faster as well as shows better accuracy.

Table 1. Selected Bands of Landsat-8 and Sentinel-2

Bands	Blue	Green	Red	NIR	SWIR1	SWIR2
Sentinel-2	B2	B3	B4	B8	B11	B12
Landsat-8	B2	B3	B4	B5	B6	B7

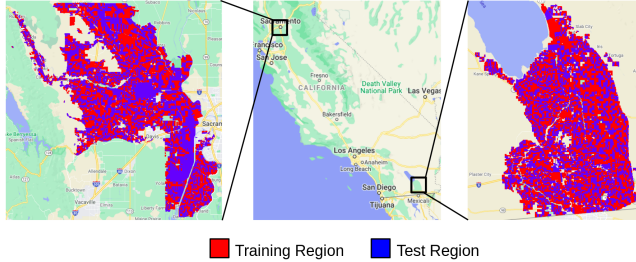


Fig. 2. The regions of interest showing training (red) and test (blue) data distribution for Yolo (left) and Imperial Counties (right) distribution.

3. RESULTS AND EVALUATION

3.1. Experimental Setup

The experiments have been performed on two different California counties, including Imperial County and Yolo County. For both regions, the crop survey data provided by the California Department of Water Resources (CDWR) [30] for the year 2016 have been used as ground truth information.

For Imperial County, 10 major classes have been considered, while 14 classes have been taken into account for Yolo County. The "Others" class contains either minor crop types, fallow land, or build up. There are about 7256 and 7340 total parcels for Imperial County and Yolo County, respectively, as mentioned in Table 2. These parcels have been split into 60% training data and 40% test data. The fields have been divided into training and test sets before sampling to ensure that no sample from the training region is included in the test set. The Fig. 2 shows the distribution of training and testing parcels. The imagery of Sentinel-2 and Landsat-8 has been used for Imperial County and Yolo County, respectively. In both cases, nine scenes from March to November 2016 have been used. The same dataset has been used to train all the classifiers, including proposed and state-of-the-art methods, in both pixel and parcel-based analysis.

3.2. Comparative Analysis

We compared our proposed hybrid model with four state-of-the-art methods, namely Random Forest, 1D CNN [15], 2D CNN[21] and 3D CNN[27]

For random forest, the number of trees has been set to 100, the minimum number of samples required to split a node is two, and the maximum number of features is set to the square root of the number of features. For the 1D Convolutional Neural Network, the architecture proposed in [15] has been used except that more features have been used instead of just EVI. The idea given by [14] has been applied to consider more features in 1D CNN. For 2D Convolutional Neural Network, five ensembles of 2D CNN have been used as proposed in [21]. The number of filters in the network ensembles is 160, 170, 180, 190, and 200. Due to the larger number of input features, more filters have to be used. For 3D Convolu-

Table 2. Summary of survey data from Imperial and Yolo counties provided by California Department of Water Resources (CDWR)

Imperial County			Yolo County		
Class	Parcels Count	%age area	Class	Parcels Count	%age area
Alfalfa	2156	31.3%	Rice	350	11.2%
Pastures	1150	15.4%	Safflower	161	2.4%
Lettuce	619	8.2%	Corn	150	2.1%
Wheat	315	4.3%	Field crops	407	6.6%
Onions	229	3.0%	Alfalfa	575	8.7%
Truck Crops	1026	11.6%	Pastures	440	4.3%
Corn	232	3.5%	Cucurbits	168	1.8%
Field Crops	192	2.9%	Tomatoes	496	9.8%
Subtropical	271	1.6%	Truck Crops	289	1.3%
Others	1066	18.2%	Almonds	799	8.9%
			Deciduous	867	5.3%
			Subtropical	176	1.1%
			Vineyard	688	5.6%
			Others	1874	30.9%

tional Neural Network, the model proposed in [27] using the concept of VGG has been used, but the number of filters has been increased to 64 and 128 in both layers. Our proposed method has the same architecture as explained in Sec. 2.

All the deep learning networks have been trained for about 50 epochs using Adam optimizer with a default learning rate of 0.001. The batch size of 128 has been used, and each network's best results have been recorded. The accuracy and weighted F1-score for each classifier are mentioned in the Tables 3. The table shows the pixel-wise accuracy and F1-score as well as the parcel-wise results. It is evident from both tables that our proposed model has outperformed all the other classifiers in both experiments. Also, other deep learning models don't show much better accuracy than the random forest, and parcel-wise accuracy for the Imperial county of random forest is greater than other deep learning models except for our proposed one. On the other hand, our 3D→1D CNN model improves the accuracy and F1-score by 2%. The parcel-wise results have been calculated by assigning each parcel a label based on the majority voting of pixels in it.

Contrary to our expectation, the parcel-wise accuracy is 4 – 5% less than pixel-wise accuracy for each classifier in the case of Yolo County. The Yolo County survey data analysis revealed that 3.5% parcels in test data were tagged as multi-use, i.e., more than one crop was sown in those fields. In contrast, Imperial County data have no field labeled as multi-use. Therefore, accuracy increased in the case of Imperial County while decreased in the case of Yolo County. Another reason is the presence of larger polygons in the test set of Yolo County.

The **Qualitative Analysis** is shown in Fig. 3 which shows the original labels from CDWR data and results produced by 3D CNN [27] and our proposed 3D→1D CNN model. In the

Table 3. Table showing comparison of our proposed 3D→1D CNN with state-of-the-art methods on Imperial and Yolo counties. The comparison is performed using pixel-wise and parcel-wise strategies (provides single classification within parcel boundary)

Classifier	Imperial County				Yolo County			
	Pixel-wise		Parcel-wise		Pixel-wise		Parcel-wise	
	Accuracy	F1-Score	Accuracy	F1-Score	Accuracy	F1-Score	Accuracy	F1-Score
Random Forest	78.96%	78.60%	80.61%	80.39%	86.68%	86.25%	82.23%	81.21%
1D CNN [15]	79.46%	79.05%	80.33%	80.24%	87.94%	87.80%	84.45%	83.90%
2D CNN [21]	79.71%	79.48%	80.54%	80.40%	88.50%	88.36%	84.55%	84.18%
3D CNN [27]	79.95%	79.70%	80.80%	80.72%	88.01%	87.82%	83.17%	82.74%
3D→1D CNN (Ours)	81.23%	81.16%	81.76%	81.76%	90.23%	90.08%	85.87%	85.51%

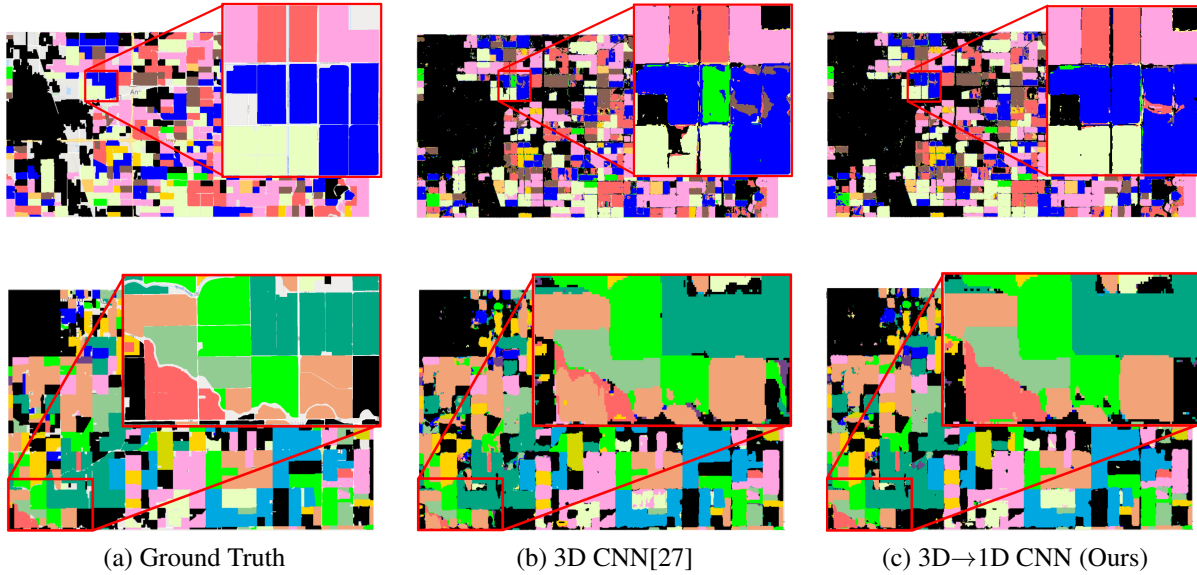


Fig. 3. Ground truth and maps produced for Imperial County (Top) and Yolo County (Bottom) by 3D CNN and our network.

figure, there are some blank spaces where ground truth was not available, and it can be observed that those blank spaces have been predicted as "Others" represented by black color. The zoomed portion of the results in Fig. 3 further illustrates that the maps produced by our hybrid model have lesser noise compared to the ones produced by vanilla 3D CNN.

Table 4. Performance Comparison of State of the art models

Classifier	Parameters	Inference time (ms)
1D CNN [15]	1,083,970	6.39
2D CNN [21]	4,278,282	7.11
3D CNN [27]	394,050	4.72
3D→1D CNN (Ours)	361,406	4.58

3.3. Computational Cost

Table 4 shows the comparison of the number of parameters in different deep learning models and their inference time. Our model has a lesser number of parameters as well as the fastest inference time. This is because, instead of flattening

the output of 3D CNN, we fed it to 1D CNN, which reduced the number of parameters and improved the performance.

4. CONCLUSION

In this paper, a new architecture and a method for large-area crop classification have been presented. Our hybrid model combines the spatio-temporal representation via 3D CNN with temporal only representation via 1D CNN. Different neural network architectures proposed in the past for crop mapping have been implemented and compared with our designed model. Experiments have been performed using multispectral imagery of different satellites to show the generality of our method. The experimentation has revealed that the proposed hybrid network performs better on benchmark CDWR datasets.

In the future, we aim to extend our approach to fields that have been marked as multi-use (having more than one crop in a small parcel) as multi-use is a more commonly observed pattern in agriculture-based economies, particularly among developing countries.

5. REFERENCES

- [1] P. Dao and Y. Liou, "Object-based flood mapping and affected rice field estimation with Landsat 8 oli and modis data," *Remote Sensing*, vol. 7, no. 5, pp. 5077–5097, 2015.
- [2] O. Csillik et al., "Object-based time-constrained dynamic time warping classification of crops using Sentinel-2," *Remote sensing*, vol. 11, no. 10, pp. 1257, 2019.
- [3] N. Kobayashi, H. Tani, X. Wang, and R. Sonobe, "Crop classification using spectral indices derived from Sentinel-2a imagery," *Journal of Information and Telecommunication*, vol. 4, no. 1, pp. 67–90, 2020.
- [4] W. Sultani A. Shakeel and M. Ali, "Deep built-structure counting in satellite imagery using attention based re-weighting," in *ISPRS Journal of Photogrammetry and Remote Sensing*, 2019.
- [5] C. Donlon et al., "The global monitoring for environment and security (gmes) Sentinel-3 mission," *Remote Sensing of Environment*, vol. 120, pp. 37–57, 2012.
- [6] M. Battude et al., "Estimating maize biomass and yield over large areas using high spatial and temporal resolution Sentinel-2 like remote sensing data," *Remote Sensing of Environment*, vol. 184, pp. 668–681, 2016.
- [7] F. Vuolo et al., "How much does multi-temporal Sentinel-2 data improve crop type classification?," *International journal of applied earth observation and geoinformation*, vol. 72, pp. 122–130, 2018.
- [8] R. Saini and SK Ghosh, "Crop classification on single date Sentinel-2 imagery using random forest and support vector machine.," *International Archives of the Photogrammetry, Remote Sensing & Spatial Information Sciences*, 2018.
- [9] P. T. Noi and M. Kappas, "Comparison of random forest, k-nearest neighbor, and support vector machine classifiers for land cover classification using Sentinel-2 imagery," *Sensors*, vol. 18, no. 1, pp. 18, 2018.
- [10] R. Sonobe et al., "An experimental comparison between kelm and cart for crop classification using Landsat-8 oli data," *Geocarto international*, vol. 32, no. 2, pp. 128–138, 2017.
- [11] R. Galiano et al., "An assessment of the effectiveness of a random forest classifier for land-cover classification," *ISPRS Journal of Photogrammetry and Remote Sensing*, vol. 67, pp. 93–104, 2012.
- [12] C. Gómez et al., "Optical remotely sensed time series data for land cover classification: A review," *ISPRS Journal of Photogrammetry and Remote Sensing*, vol. 116, pp. 55–72, 2016.
- [13] Z. Zhou, S. Li, and Y. Shao, "Crops classification from Sentinel-2a multi-spectral remote sensing images based on convolutional neural networks," in *IEEE Int. Geoscience and Remote Sensing Symposium*, 2018, pp. 5300–5303.
- [14] C. Pelletier, G. I. Webb, and F. Petitjean, "Temporal convolutional neural network for the classification of satellite image time series," *Remote Sensing*, vol. 11, no. 5, pp. 523, 2019.
- [15] L. Zhong, L. Hu, and H. Zhou, "Deep learning based multi-temporal crop classification," *Remote sensing of environment*, vol. 221, pp. 430–443, 2019.
- [16] A. M. Abdi, "Land cover and land use classification performance of machine learning algorithms in a boreal landscape using Sentinel-2 data," *GIScience & Remote Sensing*, vol. 57, no. 1, pp. 1–20, 2020.
- [17] A. Krizhevsky et al., "Imagenet classification with deep convolutional neural networks," *Advances in Neural Information Processing Systems*, vol. 25, pp. 1097–1105, 2012.
- [18] K. He, X. Zhang, S. Ren, and J. Sun, "Deep residual learning for image recognition," in *Proceedings of the IEEE Int. Conf. on Computer Vision and Pattern Recognition*, 2016, pp. 770–778.
- [19] P. Helber et al., "Eurosat: A novel dataset and deep learning benchmark for land use and land cover classification," *IEEE Journal of Selected Topics in Applied Earth Observations and Remote Sensing*, vol. 12, no. 7, pp. 2217–2226, 2019.
- [20] C. Szegedy et al., "Going deeper with convolutions," in *Proceedings of the IEEE Int. Conf. on Computer Vision and Pattern Recognition*, 2015, pp. 1–9.
- [21] K. Nataliaia et al., "Deep learning classification of land cover and crop types using remote sensing data," *IEEE Geoscience and Remote Sensing Letters*, vol. 14, no. 5, pp. 778–782, 2017.
- [22] Y. Zhou et al., "Long-short-term-memory-based crop classification using high-resolution optical images and multi-temporal sar data," *GIScience & Remote Sensing*, vol. 56, no. 8, pp. 1170–1191, 2019.
- [23] V. Mazzia, A. Khaliq, and M. Chiaberge, "Improvement in land cover and crop classification based on temporal features learning from Sentinel-2 data using recurrent-convolutional neural network (r-cnn)," *Applied Sciences*, vol. 10, no. 1, pp. 238, 2020.
- [24] G. Kwak et al., "Combining 2d cnn and bidirectional lstm to consider spatio-temporal features in crop classification," *Korean Journal of Remote Sensing*, vol. 35, no. 5_1, pp. 681–692, 2019.
- [25] M. Rußwurm and M. Körner, "Multi-temporal land cover classification with sequential recurrent encoders," *ISPRS International Journal of Geo-Information*, vol. 7, no. 4, pp. 129, 2018.
- [26] M. A. Bhimra, U. Nazir, and M. Taj, "Using 3d residual network for spatio-temporal analysis of remote sensing data," in *IEEE Int. Conf. on Acoustics, Speech and Signal Processing*, 2019, pp. 1403–1407.
- [27] S. Ji, C. Zhang, A. Xu, Y. Shi, and Y. Duan, "3d convolutional neural networks for crop classification with multi-temporal remote sensing images," *Remote Sensing*, vol. 10, no. 1, pp. 75, 2018.
- [28] M. Pal and K. Antil, "Comparison of Landsat 8 and Sentinel 2 data for accurate mapping of built-up area and bare soil," in *Asian Conf. on Remote Sensing: Space Applications: Touching Human Lives Paper*, 2017, pp. 137–140.
- [29] E. Vermote et al., "Preliminary analysis of the performance of the Landsat 8/oli land surface reflectance product," *Remote Sensing of Environment*, vol. 185, pp. 46–56, 2016.
- [30] California Department of Water Resources (CDWR), "2016 statewide crop mapping gis shapefiles," Accessed Jan. 07, 2020 [online], Available: <https://data.cnra.ca.gov/dataset/statewide-crop-mapping>.